Multirobot Multimodal Deep Sea Surveys

Use in Detailed Estimation of Manganese Crust Distribution

By Umesh Neettiyath, Harumi Sugimatsu, Tetsu Koike, Kazunori Nagano, Tamaki Ura, and Blair Thornton

©SHUTTERSTOCK.COM/MACROVECTOR

This article describes a multiyear survey of cobalt-rich manganese crust (Mn-crust) deposits using multiple underwater robots. Using two autonomous underwater vehicles and one remotely operated vehicle, mounted with camera systems, multibeam sonar, and subbottom sensors, large areas were surveyed by incorporating the advantages of each robot to create a comprehensive database of Mn-crust distribution estimates. The robots clocked in a total of 438 hours of seafloor observation, surveying about 589 km of seafloor in different locations. Specific use cases of the survey methodology and example results showing how each sensor contributes to the understanding of Mn-crust distribution are shown. The results from this survey can be combined with ship base multibeam data for seamount-scale estimates of Mn-crust volumetric distribution with high accuracy.

INTRODUCTION

The continuous advancement of technologies is driving the need for greater quantities of minerals to support innovation. Advancing technologies like electric vehicles, smartphones, and the global push for a carbon-neutral society have significantly increased the demand for batteries, which rely on essential metals, such as cobalt and nickel. As conventional land-based mineral deposits struggle to meet this escalating demand, there is a growing interest in exploring and exploiting mineral resources located on the seabed [1]. This trend is particularly crucial for island nations like Japan, which lack significant land-based mineral reserves and hence prioritize the exploration and utilization of seabed mineral resources. Primary classes of mineral deposits on the seabed are polymetallic nodules, cobalt-rich Mn-crusts, and polymetallic massive sulfides [2]. While there has been significant interest on exploring polymetallic nodules, including trial mining exercises recently, Mn-crusts have not been explored as much [3]. The exploration and extraction of seabed mineral resources are regulated by the International Seabed Authority (ISA), a subsidiary of the

United Nations. The ISA has allotted four contracts to agencies around the world for exploration of the Mn-crust for 15 years [4]. The regulations dictate that one-third of the area has to be relinquished at the end of the eighth year and 10th year each, and the final one-third of the area can be used for mineral extraction. The Japan contractor with the ISA is the Japan Organization for Metals and Energy Security (JOGMEC).

To estimate the resource potential of Mn-crusts, it is necessary to understand its formation, composition, and distribution. Mn-crusts are hydrogenetically precipitated deposits formed on hard surfaces on the seafloor [5]. They occur on the slopes and shoulders of seamounts kept free of tectonic activities for millions of years, at depths ranging from 800 m to 2,400 m, with some samples found as deep as 7,000 m. The thickness of Mn-crusts vary from a few millimeters up to 25 cm [2], although thicker Mn-crusts are very rare. The cross-sectional structure of several Mn-crust samples are shown in Figure 1, with the black top section being the Mn-crust and the brown bottom section being the substrate rock on which the crust is formed. It can be seen that the thickness can vary from a few millimeters to about 95 mm within a range of a few tens of meters. While this is a dense sampling scenario, in most practical applications, only one sample per several square kilometers is collected, which is largely insufficient to provide an accurate estimate of Mn-crust distribution.

RELATED RESEARCH

Survey of Mn-crust deposits are more difficult compared to polymetallic nodules; the former requires both the thickness and the lateral coverage to be measured, whereas the latter requires only the lateral coverage to calculate the volumetric distribution [6]. Stakeholders and researchers around the world have attempted several methods for estimating the resource potential of Mn-crusts. Since they are distributed over seamounts spanning hundreds to thousands of square kilometers, accurate estimation is a challenging task. Typically, shipboard multibeam backscatter and bathymetry data are used for estimation, combined with a near-bottom survey, such as towed video [7], remotely operated vehicle (ROV) video, ROV sidescan sonars [8], or subbottom profiler (SBP) [9]. Towed sensors and ROVs provide an output quality inferior to autonomous underwater vehicle (AUV) surveys due to the effect of tether
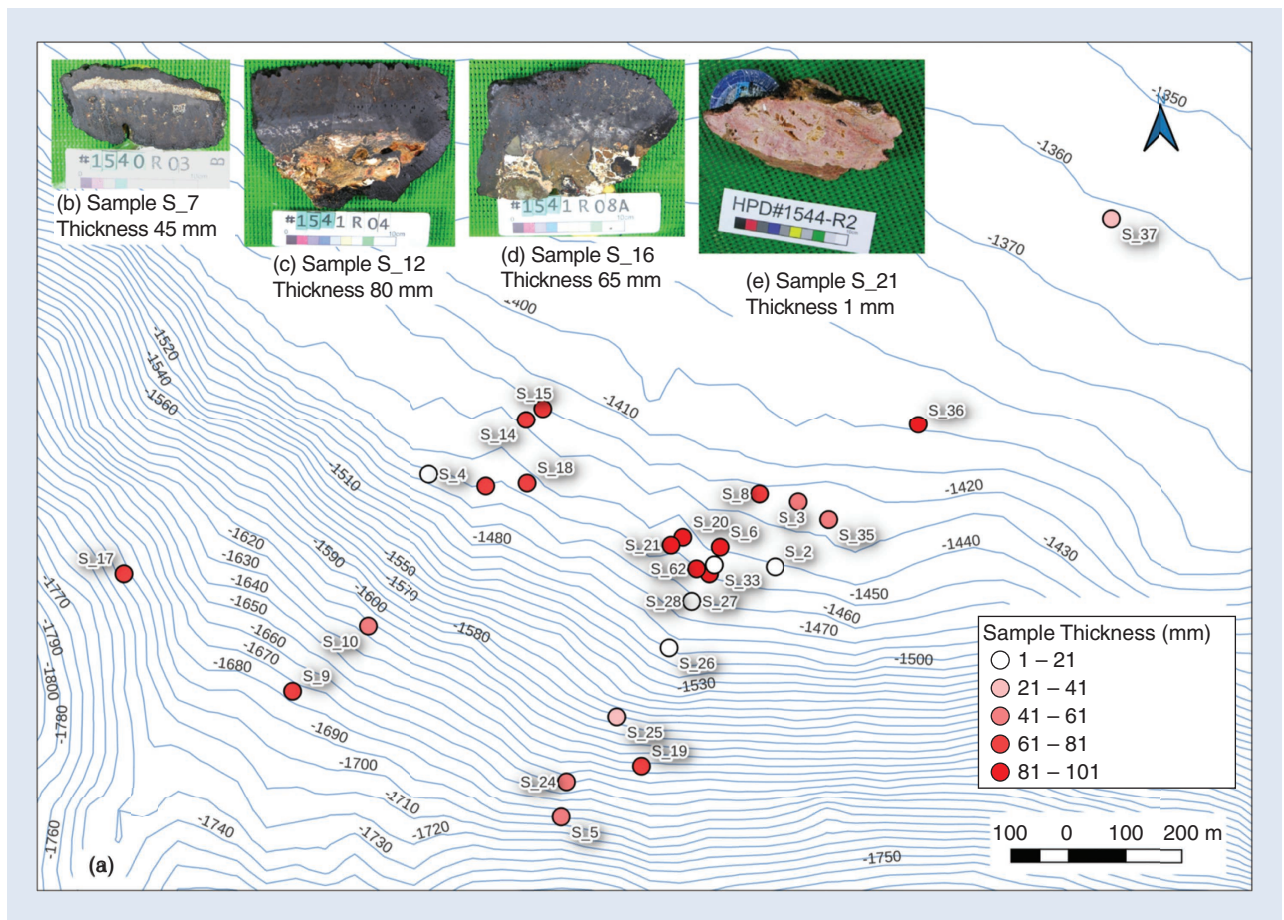

FIGURE 1. (a) Remotely operated vehicle (ROV) collected Mn-crust samples in a 2-km × 1.5-km area in the northwestern Pacific Ocean. Thirty-seven samples are shown with thickness varying from a few millimeters to 95 mm. (b)–(e) show photos of selected samples. The structure of Mn-crust, with black top section being Mn-crust and the lower section being substrate rock, can be seen. This variability of thickness was later confirmed in surveys by the autonomous underwater vehicle (AUV) Boss-A. (Data courtesy of Japan Agency for Marine Earth Science and Technology/University of Tokyo.)

forces. SBP surveys can estimate sediment layer thickness, typically with resolution of several meters, but cannot detect Mn-crust thickness or lateral coverage. All of these methods rely heavily on the visual confirmation of the seabed in a small area whose accuracy has a significant impact on the final estimates. It is therefore important to collect large ground truth datasets for more accurate resource estimation; this is one of the main themes addressed in the present work.

A robotic approach was used for polymetallic nodules estimation combining AUV-based multibeam and image surveys with ship-based multibeam surveys [10]. This survey used a single AUV over multiple dives. Multi-AUV approaches have been proposed for other applications, such as archaeological sites survey [11], although the field surveys were conducted using a single AUV. One of the motives of the present work is that by using multiple robots in tandem, we can collect more diverse multimodal data suitable for better estimation.

Thickness of the Mn-crust and its variability are equally important to the estimation. While most researchers depend on

> ## ONE OF THE MOTIVES OF THE PRESENT WORK IS THAT BY USING MULTIPLE ROBOTS IN TANDEM, WE CAN COLLECT MORE DIVERSE MULTIMODAL DATA SUITABLE FOR BETTER ESTIMATION.

physical samples collected by ROVs, dredges, or core drills for this purpose, it is expensive, time-consuming, and provides a very low spatial resolution. For example, a typical benthic multicore system, used by JOGMEC, collects a maximum of five samples during one day of operation from within a few square kilometers of area. To measure the continuous variation of thickness, the authors developed an acoustic subbottom probe for in situ measurements [12], and validated it in the area shown in Figure 1. A similar device was developed a few years later by a research team from China for surveying areas allotted to China Ocean Mineral Resources Research and Development Association [13].

In addition to increasing the spatial resolution of thickness measurements, the authors were able to combine the thickness results with simultaneously collec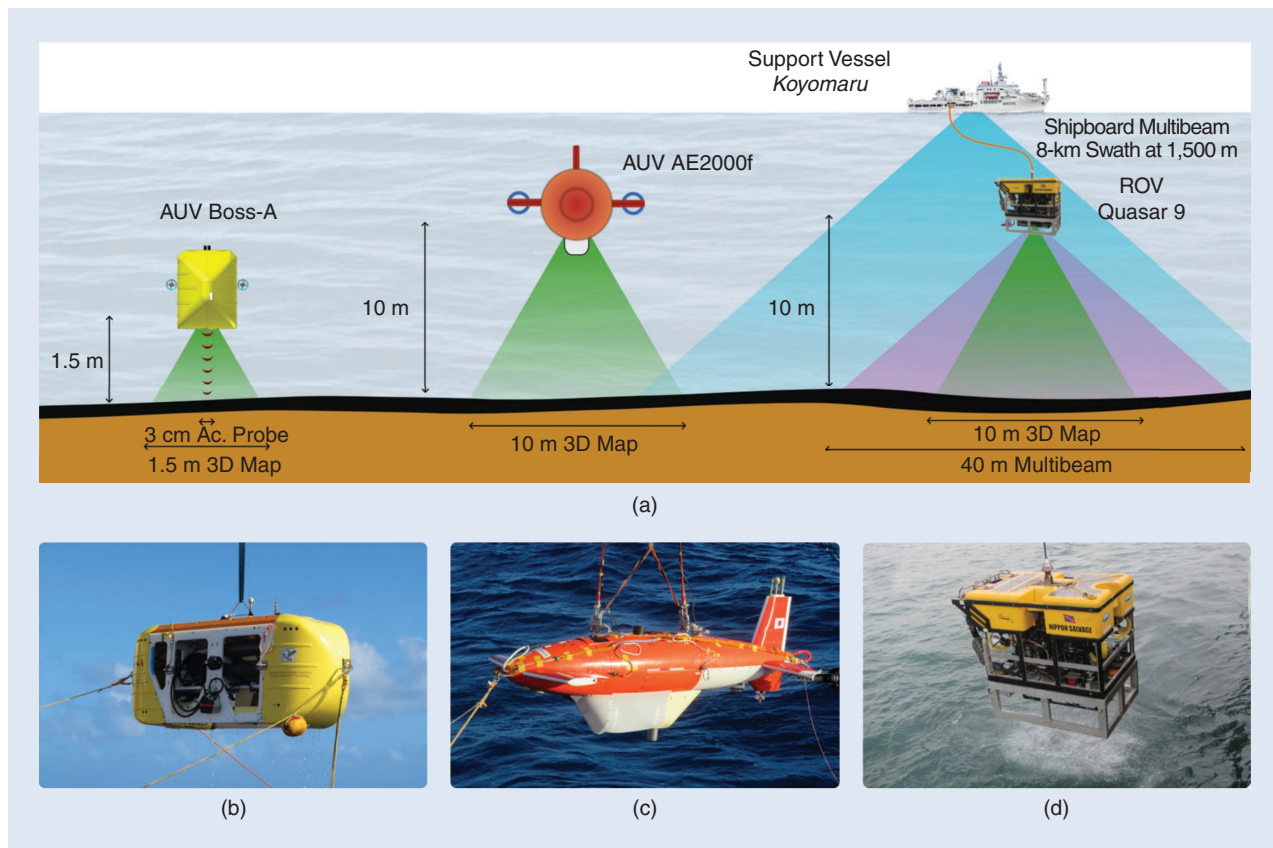ted visual mapping data to estimate volumetric distribution over hectare-scale areas by using an underwater robot [14]. These results demonstrated the utility of underwater robots—mainly AUV and ROV—for getting high accuracy Mn-crust estimates. However, the robot

FIGURE 2. (a) Conceptual overview of mapping scenario by different robots used in this survey (figure not to scale). Field deployment photos of each robot is shown below. (b) AUV Boss-A is used for Mn-crust thickness estimation and high-resolution survey. (c) AUV AE2000f is used for large area surveys. (d) ROV is used for surveying locations normally inaccessible using AUVs.

should operate close to the seafloor (1 to 2 m) for the thickness measurements, thereby limiting the lateral area visually surveyed. Hence, it is necessary to collect data from larger areas, albeit at lower resolution, which can intermediate among decameter-resolution ship-collected multibeam sonar maps with millimeter-resolution AUV-based measurements. The authors are attempting to bridge this gap by surveying using multiple robots and different sensors (multimodal) at varying resolutions, and combining the data to get higher accuracy estimates of Mn-crust distribution over seamount-scale regions.

SYSTEM OVERVIEW

A multirobot multimodal approach was used by the authors to survey Mn-crust deposits. Three robots—two AUVs and an ROV—are brought together to take advantage of the different sensors and navigational capabilities of each, as shown in Figure 2.

ROBOTS

AUV BOSS-A

This is a hovering-type AUV built in 2014 by the University of Tokyo for surveying Mn-crusts using the acoustic thickness probe. Being a hovering-type robot, it is designed to operate close to the seabed at altitudes around 1.5 m and moves slowly at .15 m/s to avoid obstacles. In addition to measuring subsurface reflections using the acoustic probe, it also creates a 3D reconstruction of the seabed using the SeaXerocks1 system. An illustration of the AUV subsystems is shown in Figure 3 and the specifications of the platform are shown in Table 1.

AUV AE2000F

This is a cruising-type AUV developed by KDDI research labs in 2001 for seafloor cable surveys. It was transferred to the University of Tokyo in 2012, renovated, and was used for high altitude (10 m) large-area mapping of the seafloor using the SeaXerocks3 seafloor mapping system. Using the streamlined shape and higher altitude from the seabed, it can operate at relatively higher speeds up to 1 m/s. It can travel up to 20 km in a single dive and can therefore cover larger areas
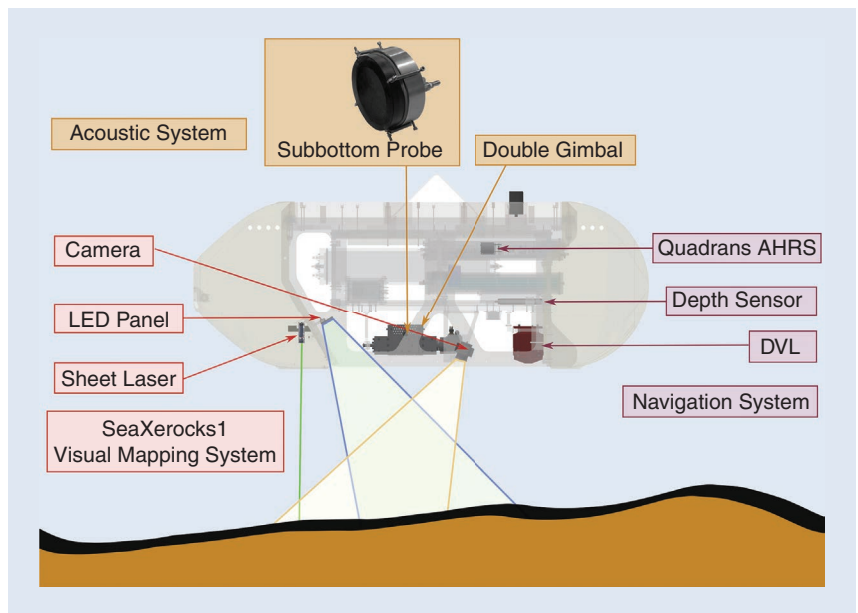

FIGURE 3. Schematic representation of Boss-A showing sensor subsystems and their components. Specifications of the AUV are shown in Table 1. AHRS: attitude heading reference system; DVL: Doppler velocity log.

TABLE 1. Specifications of the platform (AUV Boss-A).

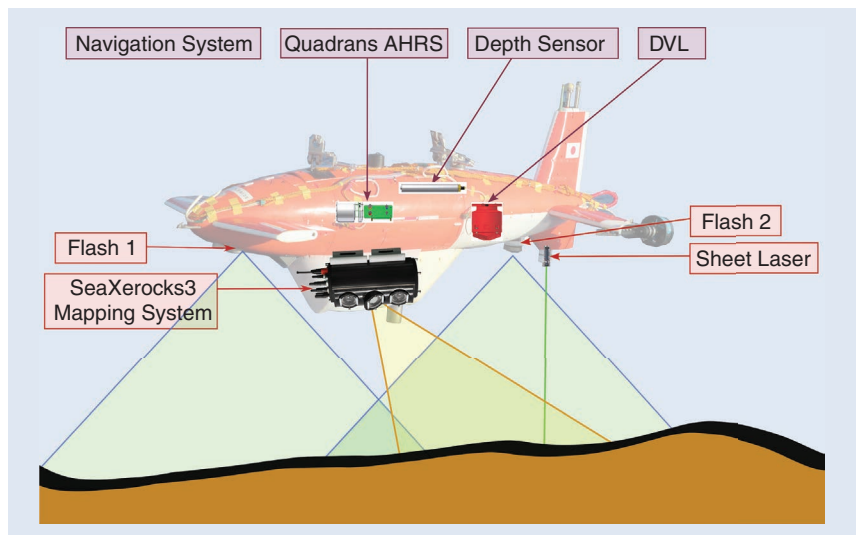| DIMENSIONS	3 M × 1.15 M × 1.25 M
Mass	580 kg
Operating velocity	.3 kn (.15 m/s)
Operating altitude range	1.5 ± .5 m
Depth rating	3,000 m
Endurance	7 h
Payloads	Acoustic thickness probe
	SeaXerocks1 mapping system

FIGURE 4. Schematic representation of AE2000f showing sensor subsystems and their components. Specifications of the AUV are shown in Table 2.

compared to the other robots. An illustration of the AUV subsystems is shown in Figure 4. Specifications of the AUV AE2000f platform are shown in Table 2.

ROV QUASAR9

This is a work-class 3,000-m rated ROV owned and operated by Nippon Salvage Co. Ltd. In the payload section of the ROV, sensors for surveying the seafloor were attached, as shown in Figure 5. Since the ROV is manually operated, it could traverse more rugged terrain, such as cliffs and steep sections of the seabed. Although existence of Mn-crust deposits in such regions is known, these areas are avoided by AUVs due to operational safety. The ROV operates at an altitude of about 10 m from the seafloor, generating 3D maps of centimeter-order resolution using the SeaXerocks3 system. The visual 3D mapping and navigational components are the same as the ones installed in AE2000f. The power and communications are obtained through the ROV tether cable. However, unlike the AUVs, the ROV data are monitored and adjustments made in real time using a visualization software from the shipboard control room. Specifications of the ROV QUASAR9 platform are shown in Table 3.

SENSOR SYSTEMS

Specifications of the sensor systems used are provided in Table 4. These sensors are paired with a navigation system, which consists of the AUV's navigational sensors. These include an iXblue Quadrans attitude heading reference system (AHRS) for pose estimation, Doppler velocity log (DVL) for self-localization, paroscientific pressure sensor for depth measurement, and an iXblue GAPS system for localization from the support vessel.

ACOUSTIC PROBE FOR THICKNESS

Acoustic probe for thickness is a parametric sonar that records subsurface reflections of the seafloor for estimating the Mn-crust thickness [12]. The probe consists of a five-channel

TABLE 2. Specifications of the platform (AUV AE2000f).

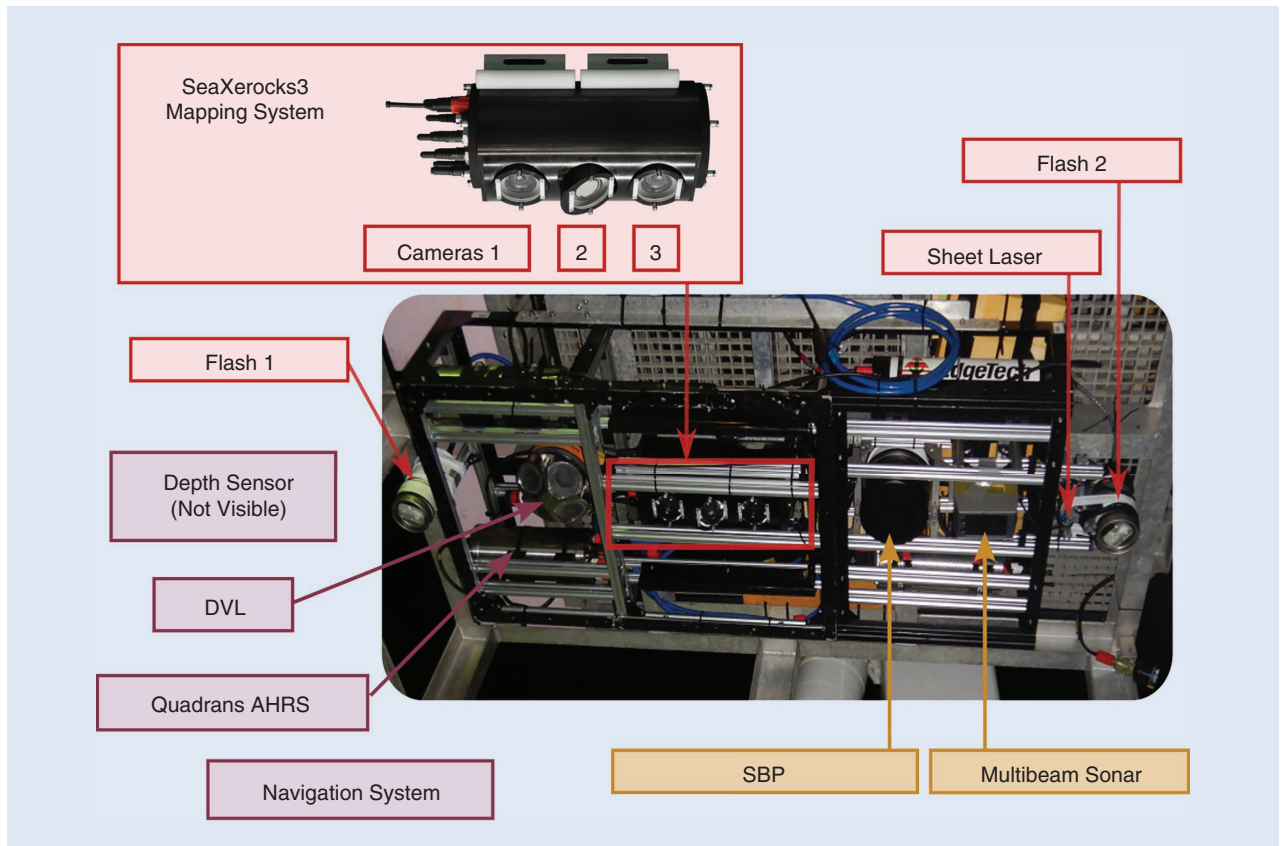| DIMENSIONS	3 M × 1.3 M × .9 M
Mass	370 kg
Operating velocity	2 kn (1 m/s)
Operating altitude range	10 ± 2 m
Depth rating	2,000 m
Endurance	6 h
Payloads	SeaXerocks3 mapping system

FIGURE 5. For surveys using the ROV, the sensors were mounted on a payload skid installed at the bottom of the robot. The visual 3D mapping and navigational components are same as the ones installed in AE2000f. In addition, a multibeam sonar is installed for simultaneous wide-area acoustic survey. SBP: sub-bottom probe.

annular array of 2-MHz piezoelectric transducers for transmission and a 200-kHz piezoelectric transducer to record reflections. It is dynamically focused on the seafloor at ranges from .5 to 2.5 m. Since optimal measurements require the probe to be orthogonal to the measured surface, the probe is mounted on a two-axis gimbal. Using the SeaXerocks1 visual mapping system, the relative slope of the seafloor is calculated in real time and the gimbals are oriented normal to the seafloor [15]. The signals are analyzed to remove noise, to find reflections from the crust–substrate boundary, to determine continuity of measurements, and to calculate the thickness values using the method described in [14].

SEAXEROCKS1 MAPPING SYSTEM

The SeaXerocks1 mapping system is used for low-altitude (1.5 m) survey in this project, and is integrated into the AUV Boss-A for simultaneous mapping of the seafloor together with the acoustic probe. This system is a light-sectioning–based seafloor 3D mapping system consisting of a sheet laser, LEDs for illumination, and a camera that records the laser projection on the seafloor and generates visual color reconstructions of the seafloor.

SEAXEROCKS3 MAPPING SYSTEM

The SeaXerocks3 mapping system is used for high-altitude (10 m) surveys in this project [16]. It consists of three cameras: a stereo pair for color imaging of the seafloor and a monochrome camera for recording the laser projection on the seafloor. The system can produce 3D reconstructions of the seafloor in two methods. The first method is similar to SeaXerocks1, with the exception of using separate cameras for laser bathymetry and color detection. The second method uses feature matching from the stereo camera images.

MULTIBEAM SONAR

Multibeam sonar is used for wide-area acoustic observation of the seafloor from the ROV. The authors used an Imagenex

TABLE 3. Specifications of the platform (ROV QUASAR9).

DIMENSIONS	3.2 M × 1.8 M × 1.8 M
Mass	3,500 kg
Payload mass	250 kg
Operating velocity	.2 kn (.1 m/s)
Operating altitude range	10 ± 2 m
Depth rating	3,000 m
Umbilical cable length	3,200 m
Manipulators	five-axis and seven-axis
Payloads	High-vision camera
	Multibeam sonar
	Sub Bottom Probe
	SeaXerocks3 mapping system

TABLE 4. Specifications of the sensors used.

SENSOR TYPE	SPECIFICATION
Acoustic thickness probe	
Type	Parametric subbottom sonar
Frequency	2 MHz (carrier), 200 kHz (signal)
–3 dB footprint	<2 cm (dynamic focusing)
Mounting	Two-axis gimbal
Gimbal roll, pitch range	±15°, ±45°
Ping rate	20 Hz
SeaXerocks1 3D visual mapping system	
Type	Monocular vision and
	Structured light using sheet laser
Illumination	2× LED panels (20,000 lm/panel)
Laser power, wavelength	120 mW, 532 nm
Camera resolution, FOV	1,328 × 1,048, 65°× 53°
Camera frame rate	15 fps
Laser to camera baseline	1.22 m
Swath, resolution	1.5 m, 1.4 mm
Bathymetry resolution (at 1.5 m)	1.4 mm (cross-transect)
	6.7 mm (along-transect)
	3.0 mm (depth)
SeaXerocks3 3D visual mapping system	
Type	Stereo vision and
	Structured light using sheet laser
Illumination	2× Xenon flash lamps
Laser power, wavelength	120 mW, 532 nm
Camera resolution, field of view	1,280 × 1,024, 68° × 57°
Camera frame rate	.2 fps (stereo)
	10 fps (bathymetry)
Swath, resolution	10 m, 9 mm
Bathymetry resolution (at 10 m)	9 mm (cross-transect)
	20 mm (along-transect)
	87 mm (depth)
Imagenex Delta-T 837B sonar	
Type	Multibeam sonar
	Bathymetry and backscatter
Frequency	260 kHz
Transducer Beam Width	120 × 3
Number of beams	120
Beam resolution	1°
Horizontal opening angle	120°
Minimum Range	.5 m
Range resolution	.02 % of range
Frame rate	12 Hz
Swath (at 10-m altitude)	40 m
Bathymetry resolution (at 10 m)	333 mm (cross-transect)
	20 mm (along-transect)
	20 mm (depth)

TABLE 5. Summary of dives conducted over five years.

ROBOT		2018	2019	2020	2021	2022	TOTAL	AVERAGE (PER DIVE)
	No. of dives	5	5	4	9	5	28	—
AE2000f	Total length (km)	71.8	55.6	53.8	105.3	92.3	378.8	13.5
	Total duration (hh:mm)	19:54	27:15	21:15	42:17	7:21	141:50	5:03
	No. of dives	6	1	3	2	1	13	—
Boss-A	Total length (km)	18.3	3.1	8.1	3.8	2.5	35.8	2.8
	Total duration (hh:mm)	25:50	4:43	11:53	5:56	3:28	51:50	3:59
	No. of dives	11	7	5	12	6	41	—
ROV	Total length (km)	47.9	33.7	16.0	58.9	18.3	174.8	4.3
	Total duration (hh:mm)	59:54	48:39	28:39	69:22	38:30	245:04	5:58

By alternatively operating ROVs and AUVs, multiresolution, multimodal data could be collected over large areas of Mn-crust deposits in a variety of landscapes.

Model 837B Delta T multibeam imaging sonar with 120 beams resolved digitally. It was controlled from a dedicated beamforming software running over an ethernet link. Recorded data are postprocessed to generate bathymetry and backscatter maps of the surveyed seafloor. The difference in backscatter intensity between hard and soft surfaces can be used to identify Mn-crust covered areas from sediment covered areas.

FIELD SURVEYS

Several surveys were conducted over five years using the described systems to estimate the distribution of Mn-crust resources in the northwest Pacific Ocean, offshore of Minami Torishima Island at depths ranging from 1,000 m to 2,000 m below sea level. A summary of the dives by each robot is given in Table 5.

SURVEY METHODOLOGY

Target survey locations were decided based on shipboard multibeam maps and previous surveys. Depending on the location, one or more robots were chosen to conduct the survey. Visual confirmation of the Mn-crust was conducted mostly using the AE2000f, with the ROV being used for more rugged areas. Close-up high-resolution surveys and thickness measurements were done using the Boss-A in areas where Mn-crust is confirmed or highly probable. Multiresolution surveys were conducted in the same area using multiple robots for correlating multimodal data.

The robots surveyed the seafloor by following predefined waypoints by keeping a constant altitude. The waypoints were arranged in different modes of survey: line transect, dense grids, or sparse grids. With a wide swath of 10 m, dense grid surveys are better realized with the AE2000f. While it is
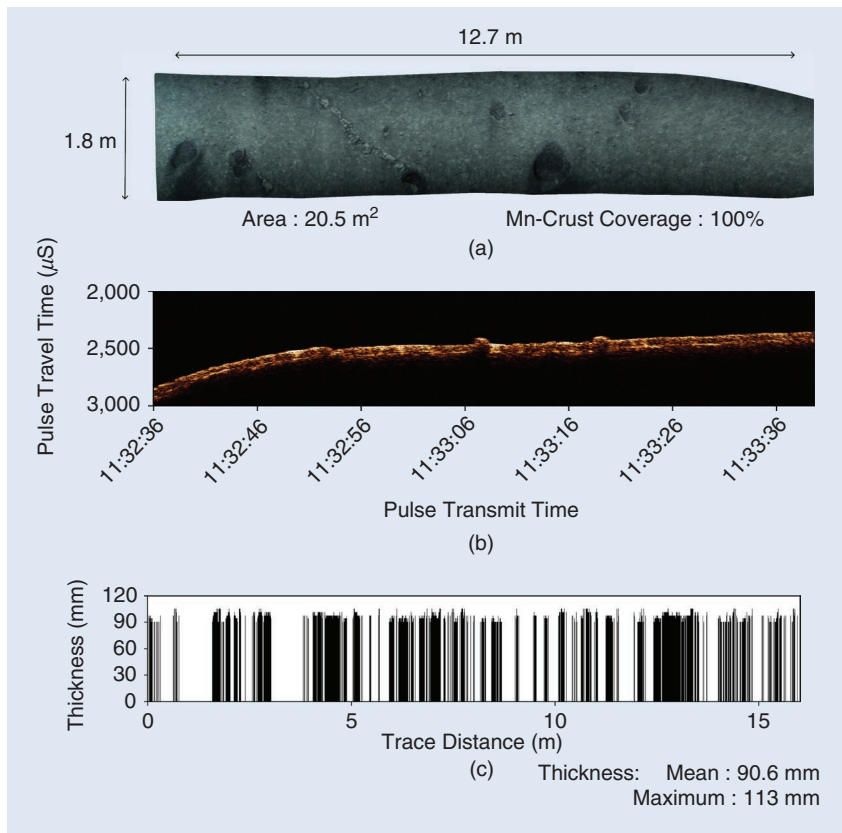

FIGURE 6. Thickness estimations by Boss-A. (a) Seafloor reconstruction showing a flat Mn-crust area. (b) Acoustic reflections. Primary and secondary reflections are sharper than most places, albeit discontinuous. (c) Estimated thickness values. The gaps denote areas where the thickness calculation is not performed due to data inconsistency or absence of Mn-crust.

possible to do dense grid surveys with Boss-A with a narrow swath of 1.5 m, the area covered is of the order of only a few hundred square meters. Sparse grids can be done with either AUV. ROVs are manually operated and therefore produce undulations in the positioning, causing a mapping output of a lower quality. Therefore, the ROV transects were generally connected straight-line segments.

All robots were tracked during operation using an ultrashort baseline (USBL) system on the survey vessel. Real-time navigation of AUVs is based on dead reckoning-based self-localization using a DVL, combined with the AHRS. The ROV was operated by pilots monitoring the USBL real-time position. Both AUVs are equipped with an acoustic modem for communicating with the survey ship. Due to the low bandwidth, it is only used for telemetry and emergency signaling. To optimize the use of valuable ship time and resources, operations were conducted around the clock by several teams of researchers.

DATA ANALYSIS

The data collected by each robot is analyzed postdive. The navigational systems used have two types of uncertainties, drift and bias, both highly dependent on the environmental conditions. Inertial navigation sensors (DVL and AHRS) drift over time, causing the robot to move away from the desired trajectory and is typically less than 2% of traveled distance. The bias occurs in the USBL tracking system for global positioning, is random in nature, and can be up to 1% of slant range (straight-line distance from the ship to the robot). In the case of a survey at 1,500-m depth, this amounts to about 15 m, more than the width of high-altitude visual surveys. We have used an extended Kalman filter in postprocessing to combine the inertial navigation sensors with the USBL system to minimize the error, and this position estimate is used for map generation.

In the case of the Boss-A, the 3D maps generated by the Boss-A are classified by using a support vector machine classifier into continuous Mn-crust deposits, Mn-nodules and sediments, and an estimate of the percentage cover of exposed Mn-crust is calculated [14]. In areas identified as Mn-crust, the acoustic subsurface reflections were analyzed to calculate thickness values, as shown in Figure 6. By extrapolating the thickness results to the entire 3D map, volumetric estimates are generated. Using the density of Mn-crust calculated from samples collected in the past, estimates are made for the mass coverage per unit area; for example, the area shown in Figure 6 has a mass coverage of 174 kg/m^2.
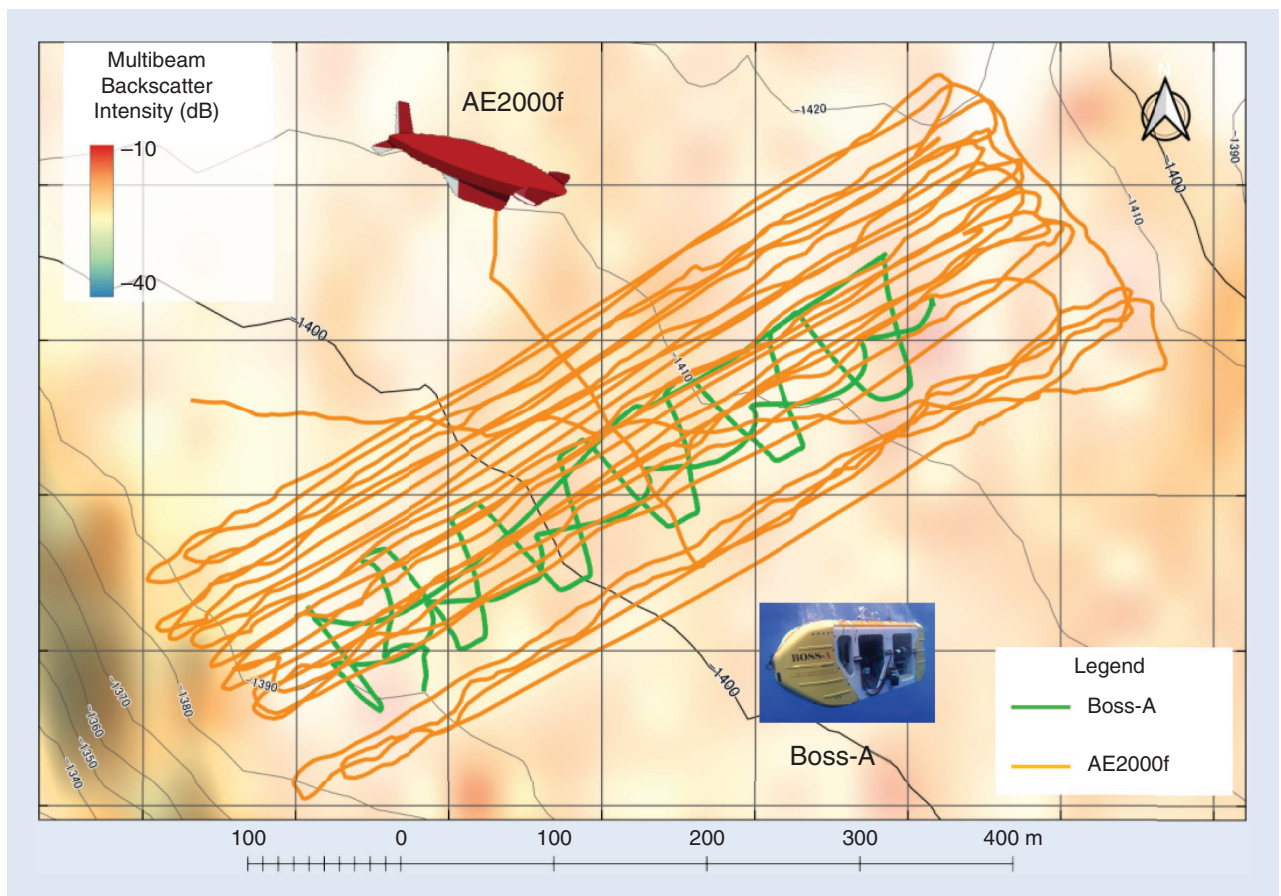

FIGURE 7. Navigation tracks of the AUVs (orange) AE2000f and (green) Boss-A at one of the surveyed locations. The survey results are shown in Figures 8 and 9.

In the case of the AE2000f and ROV using the SeaXerocks3 system, the 3D reconstruction is generated using one of the two methods mentioned in the "SeaXerocks3 Mapping System" subsection. Simultaneously, the images were classified using a semisupervised location-guided autoencoder to classify the seafloor and generate percentage cover estimates [18].

RESULTS

Figure 7 shows a case study that shows the benefits of the proposed methodology. Initially, the AE2000f conducted a dense grid survey of the area, 210 m × 620 m, in a lawn-mower pattern with a total length of 17.7 km in 4:40 hours. Since large Mn-crust deposits were identified in camera images, Boss-A was deployed in the subsequent dive to conduct a sparse grid survey, 462 m × 82 m, with a total length of 2.3 km in 3:30 hours. The navigation transects are shown in Figure 7 and the 3D reconstructions generated are shown in Figure 8. Different types seafloor, including flat Mn-crusts, pillowy Mn-crusts, and nodules are visible in this area, with co-located maps from the two robots showing similar landscapes. Figure 8(b) and (c)

show zoomed views highlighting the tradeoff between swath and resolution.

Further analysis of Boss-A data are done to generate highly accurate volumetric estimates of Mn-crust in the surveyed area, as shown in Figure 9. The results showed a thickness of 74 ± 27 mm. Of the 2,779 m^2 area surveyed, 80% is covered with Mn-crust with a unit mass coverage of 120 kg/m^2.

Figure 10 shows a section of the data collected by the ROV, consisting of alternating sections of rocky Mn-crust and sediment deposits. It can be seen that the multibeam backscatter can identify areas containing Mn-crusts for an area three times that of the visually surveyed area. The seafloor matches between the visual and sonar surveys. However, low acoustic backscatter intensity alone is not always a good indicator of the absence of Mn-crust due to the presence of buried Mn-crust layers in some areas.

DISCUSSION AND FUTURE WORK

The authors faced several challenges while collecting and analyzing this large dataset. Excluding the operational challenges, such as bad weather conditions, instrument failures,
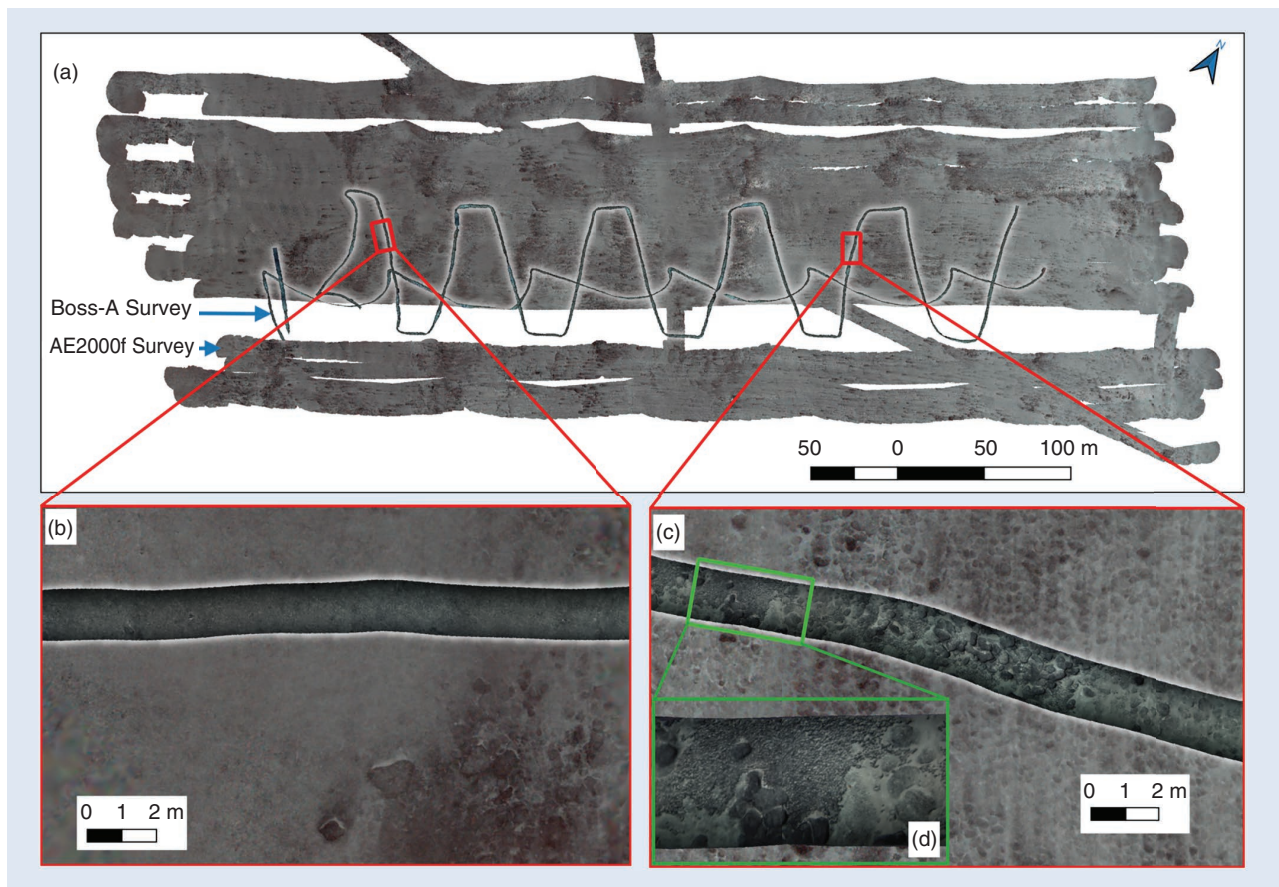

Boss-A Survey
AE2000f Survey

FIGURE 8. (a) Top view of 3D maps of a Mn-crust covered area generated by AE2000f (outer image) and Boss-A (inner image, highlighted for better visibility). (b) Close-up view of a flat Mn-crust area. (c) Close-up view of a flat Mn-crust area with pillowy sections. (d) Further close-up view of the Boss-A map show small nodules, almost invisible in AE maps. With narrow-swath millimeter-resolution Boss-A maps, small features can be seen, whereas with wide swath, centimeter-resolution AE maps, larger areas can be studied. In addition, Boss-A can study the subsurface structure of Mn-crust and measure its thickness and volumetric coverage, as shown in Figure 9.

and human errors, some of the technical challenges are discussed below.

Localization among multiple surveys is difficult and an exact match of position is not obtained because the map width (1.5 m or 10 m) is much lower than the positioning error of the USBL system (about 15 m or 1% of slant range), making the same point having an offset up to 30 m between surveys. An extended Kalman filter can create navigation solutions suitable for 3D mapping purposes, but the results from different days of survey will have an unknown offset. Currently, these are adjusted manually; localization solutions based on image matching, by adapting a stereo matching solution [17] for multirobot surveys, is a potential solution.

Multibeam reflection is strongly affected by the beam geometry with the central beams having stronger backscatter intensities. It is possible to minimize this by reducing the
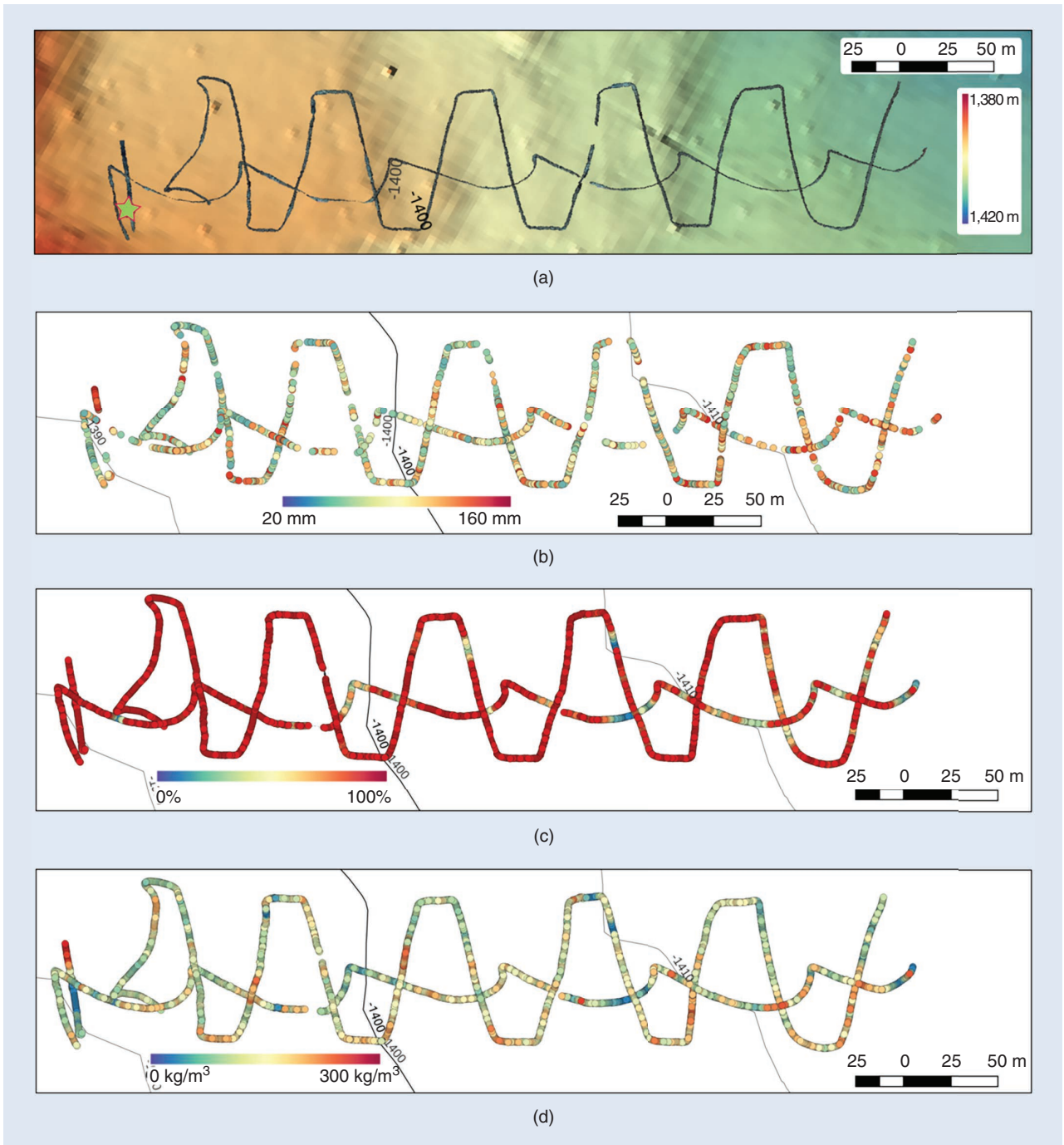

FIGURE 9. Volumetric estimates of Mn-crust calculated from the data collected by Boss-A. (a) Top view of the 3D mosaic generated, with the bathymetric map generated by AE2000f in the background. (b) Calculated thickness values. (c) Percentage cover of exposed Mn-crust deposits. Since the area shown is a large flat Mn-crust deposit, the coverage is close to 100% in most areas. (d) Unit mass coverage. The star indicates the location of the patch shown in Figure 6.

transmitted signal power, but this has the effect of weaker reflections from the outer beams and limiting the effective coverage. This was compensated by beam correction using an angle-dependent attenuation function; nevertheless, some artifacts remain.

In SeaXerocks1 and SeaXerocks3, the images are preprocessed individually to correct the lens distortion and light attenuation in the seawater. Mathematical models for light transmission and attenuation in seawater for each color channels is used to correct the color of images. Another method is to balance the grey levels for each pixel in the image across the entire image dataset, assuming a uniform illumination scenario. These models still need to be tuned for each dataset for the best results.

Analyzing the large amounts of data collected is also a daunting task. Automated analysis methods utilizing machine learning tools can significantly reduce the workload and reduce the time taken, while increasing the output quality [14], [18]. However, training and validating the systems needs ground truth data, which is difficult to obtain in deep sea environments. Therefore, multimodal sensor data are compared to each other for better understanding and validation.

Artificial intelligence models tuned to regions from one area may not work as efficiently in other areas due to changing conditions. Increasing the robustness of these models is a potential research problem. New methods for synergistically combining multimodal, multiresolution data for seamount scale (hundreds to thousands of square kilometers) areas is another research theme being actively pursued. Sensor-agnostic methods of correlating multimodal data are being considered for this task.

One of the highlights of this survey was the ability to identify Mn-crust deposits buried under thin layers of sediment (<30-cm thick), using the Boss-A's acoustic probe. While sonar and visual mapping surveys notice only sediment, Boss-A could identify buried layers, which were assumed to be Mn-crust, based on surrounding areas. These results were later validated using benthic multicore system sampling [19].

The authors could study the variability of Mn-crust distribution both within the same seamount and across different seamounts. It was observed that the variability depends on the choice of location and general trends can be deceptive, further reinforcing the need of similar surveys.

Although the system proposed is used for Mn-crust surveys, they can be used for other seafloor surveys as well by changing the sensor suite. For example, polymetallic nodules can be surveyed without using the acoustic thickness probe. By adding methane or other chemical sensors, methane seeps and hydrothermal vents can be surveyed. The number and choice of robots was made by considering features of the Mn-crust deposits. While reducing the number of robots will negatively impact the results, increasing the number of robots with other sensors can have a positive impact. In particular, collecting high-altitude sidescan sonar, and/or multibeam surveys from a cruising AUV at 30- to 60-m altitude can provide wider area survey results, adding an additional resolution level to improve the prediction accuracy. Efforts in this direction are ongoing.

Although this study used multiple robots, they were not operating simultaneously or as a coordinated multiagent system. While this is a future direction of underwater robotics, several challenges, including localization and communication, need to be addressed before it can be realized in the deep sea field surveys.
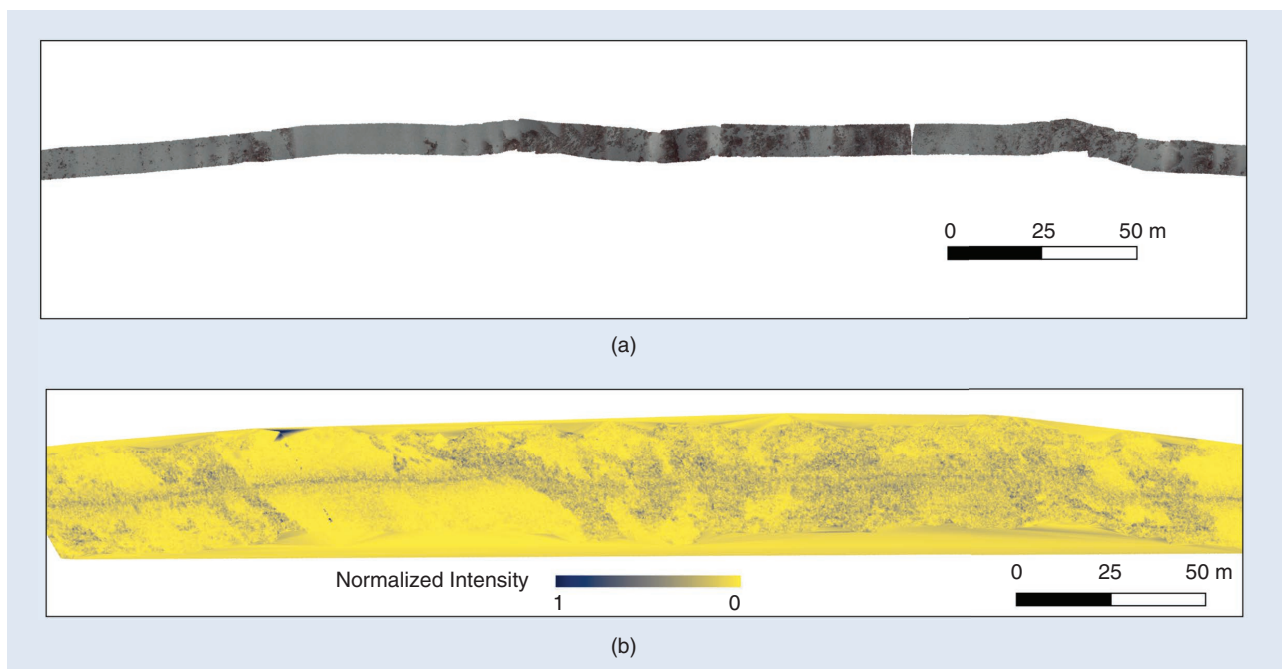

FIGURE 10. Example of data collected by the ROV. (a) Top view of 3D reconstruction and (b) multibeam backscatter data. It can be clearly seen that albeit at a lower resolution, the multibeam can distinguish between the Mn-crust and sediment covered areas for a larger area surrounding the visual 3D map.

CONCLUSION

The authors have conducted a multirobot multimodal survey of deep sea Mn-crust resources over a period of five years and have presented a portion of the results. By utilizing the advantages of each system, a variety of data regarding the thickness, exposure coverage, and mass coverage of Mn-crust were collected. Descriptions of systems used, survey strategies, data analysis methodologies, and considerations for future work are discussed.

Mn-crust exploitation is still technologically not feasible and economically not viable [20]. While technology improves the feasibility of deep-sea mineral exploitation of deep-sea mineral exploitation, other issues, such as the effect on the ecosystem, pollution, and effect on marine animals must be addressed. These studies have not yet picked this up. Nevertheless, robotic surveys, such as the present work, are important both in terms of technology development, the dataset collected, and scientific relevance for studying these deep sea environments.

ACKNOWLEDGMENT

AUTHORS

Umesh Neettiyath, Institute of Industrial Science, University of Tokyo, Tokyo 153-8505, Japan. E-mail: umesh@iis.u-tokyo.ac.jp.

Harumi Sugimatsu, Institute of Industrial Science, University of Tokyo, Tokyo 153-8505, Japan. E-mail: harumis@iis.u-tokyo.ac.jp.

Tetsu Koike Kaiyo Engineering Co., Ltd., Tokyo 110-0016, Japan, and the Institute of Industrial Science, University of Tokyo, Tokyo 153-8505, Japan. E-mail: koike@kaiyoeng.com.

Kazunori Nagano, Institute of Industrial Science, University of Tokyo, Tokyo 153-8505, Japan, and IDEA Consultants, Inc., Tokyo 154-8585, Japan. E-mail: k-nagano@iis.u-tokyo.ac.jp.

Tamaki Ura, Institute of Industrial Science, University of Tokyo, Tokyo 153-8505, Japan. E-mail: ura@iis.u-tokyo.ac.jp.

Blair Thornton, Marine Autonomy, University of Southampton, SO16 7QF Southampton, U.K., and Institute of Industrial Science, University of Tokyo, Tokyo 153-8505, Japan. E-mail: b.thornton@soton.ac.uk.

REFERENCES

[1] J. R. Hein, K. Mizell, A. Koschinsky, and T. A. Conrad, "Deep-ocean mineral deposits as a source of critical metals for high- and green-technology applications: Comparison with land-based resources," *Ore Geol. Rev.*, vol. 51, pp. 1–14, Jun. 2013, doi: 10.1016/j.oregeorev.2012.12.001.

[2] P. A. J. Lusty and B. J. Murton, "Deep-ocean mineral deposits: Metal resources and windows into earth processes," *Elements*, vol. 14, no. 5, pp. 301–306, Oct. 2018, doi: 10.2138/gselements.14.5.301.

[3] E. Baker and Y. Beaudoin, Eds., *Deep Sea Minerals: Cobalt-Rich Ferromanganese Crusts, a Physical, Biological, Environmental, and Technical Review*. Noumea, New Caledonia: Secretariat of the Pacific Community, 2013.

[4] "Regulations on prospecting and exploration for cobalt-rich ferromanganese crusts in the area," International Seabed Authority, Kingston, Jamaica, ISBA/17/C/CRP.1, Oct. 2012. [Online]. Available: https://digitallibrary.un.org/record/733356

[5] A. Usui et al., "Continuous growth of hydrogenetic ferromanganese crusts since 17 Myr ago on Takuyo-Daigo Seamount, NW Pacific, at water depths of 800–5500 m," *Ore Geol. Rev.*, vol. 87, pp. 71–87, Jul. 2017, doi: 10.1016/j.oregeorev.2016.09.032.

[6] M. M. P. Weydert, "Measurements of the acoustic backscatter of selected areas of the deep seafloor and some implications for the assessment of manganese nodule resources," *J. Acoustical Soc. Amer.*, vol. 88, no. 1, pp. 350–366, Jul. 1990, doi: 10.1121/1.399910.

[7] J. Joo et al., "Seabed mapping using shipboard multibeam acoustic data for assessing the spatial distribution of ferromanganese crusts on seamounts in the Western Pacific," *Minerals*, vol. 10, no. 2, pp. 1–20, 2020, doi: 10.3390/min10020155.

[8] J. Kim, Y.-T. Ko, K. Hyeong, and J.-W. Moon, "Geophysical and geological exploration of cobalt-rich ferromanganese crusts on a seamount in the Western Pacific," *Econ. Environmental Geol.*, vol. 46, no. 6, pp. 569–580, 2013, doi: 10.9719/EEG.2013.46.6.569.

[9] B. Zhao et al., "Sedimentary characteristics based on sub-bottom profiling and the implications for mineralization of cobalt-rich ferromanganese crusts at Weijia Guyot, Western Pacific Ocean," *Deep Sea Res. I, Oceanogr. Res. Papers*, vol. 158, Apr. 2020, Art. no. 103223, doi: 10.1016/j.dsr.2020.103223.

[10] E. Alevizos, T. Schoening, K. Koeser, M. Snellen, and J. Greinert, "Quantification of the fine-scale distribution of Mn-nodules: Insights from AUV multi-beam and optical imagery data fusion," *Biogeosciences Discuss..*, Feb. 2018. Accessed: Oct. 30, 2023. [Online]. Available: https://bg.copernicus.org/preprints/bg-2018-60/

[11] J. Wu et al., "Multi-AUV motion planning for archeological site mapping and photogrammetric reconstruction," *J. Field Robot.*, vol. 36, no. 7, pp. 1250–1269, Oct. 2019, doi: 10.1002/rob.21905.

[12] B. Thornton, A. Asada, A. Bodenmann, M. Sangekar, and T. Ura, "Instruments and methods for acoustic and visual survey of manganese crusts," *IEEE J. Ocean. Eng.*, vol. 38, no. 1, pp. 186–203, Jan. 2013, doi: 10.1109/JOE.2012.2218892.

[13] F. Hong, H. Feng, M. Huang, B. Wang, and J. Xia, "China's first demonstration of cobalt-rich manganese crust thickness measurement in the Western Pacific with a parametric acoustic probe," *Sensors*, vol. 19, no. 19, 2019, Art. no. 4300, doi: 10.3390/s19194300.

[14] U. Neettiyath et al., "Deep-sea robotic survey and data processing methods for regional-scale estimation of manganese crust distribution," *IEEE J. Ocean. Eng.*, vol. 46, no. 1, pp. 102–114, Jan. 2021, doi: 10.1109/JOE.2020.2978967.

[15] T. Sato, B. Thornton, A. Bodenmann, A. Asada, and T. Ura, "Towards real-time control of a double gimbaled acoustic probe for measurement of manganese crusts thickness," in *Proc. IEEE Int. Underwater Technol. Symp. (UT)*, Mar. 2013, pp. 1–5, doi: 10.1109/UT.2013.6519880.

[16] B. Thornton et al., "Biometric assessment of deep-sea vent megabenthic communities using multi-resolution 3D image reconstructions," *Deep Sea Res. I, Oceanogr. Res. Papers*, vol. 116, pp. 200–219, Oct. 2016, doi: 10.1016/j.dsr.2016.08.009.

[17] M. Johnson-Roberson, O. Pizarro, S. B. Williams, and I. Mahon, "Generation and visualization of large-scale three-dimensional reconstructions from underwater robotic surveys," *J. Field Robot.*, vol. 27, no. 1, pp. 21–51, Jan./Feb. 2010, doi: 10.1002/rob.20324.

[18] T. Yamada, A. Prügel-Bennett, and B. Thornton, "Learning features from georeferenced seafloor imagery with location guided autoencoders," *J. Field Robot.*, vol. 38, no. 1, pp. 52–67, Jan. 2021, doi: 10.1002/rob.21961.

[19] U. Neettiyath, B. Thornton, H. Sugimatsu, T. Sunaga, J. Sakamoto, and H. Hino, "Automatic detection of buried Mn-crust layers using a sub-bottom acoustic probe from AUV based surveys," in *Proc. IEEE/MTS Oceans*, Chennai, India, 2022, pp. 1–7, doi: 10.1109/OCEANSChennai45887.2022.9775260.

[20] T. Yamazaki, N. Nakatani, and R. Arai, "An economic feasibility analysis for combined mining of cobalt-rich crusts and phosphorous ores in north-west pacific," in *Proc. IEEE Underwater Technol. (UT)*, Tokyo, Japan, Mar. 2023, pp. 1–4, doi: 10.1109/UT49729.2023.10103423.